Progress In Electromagnetics Research C, Vol. 158, 47–55, 2025

PIER C

(Received 14 June 2025, Accepted 18 July 2025, Scheduled 1 August 2025)

Design of a Single-Layer Filtering Patch Antenna with High Gain

Zhonggen Wang[1], Hao Gui[1,*], Wenyan Nie[2], Ming Yang[3], and Chenlu Li[4]

[1] *School of Electrical and Information Engineering, Anhui University of Science and Technology, Huainan 232001, China*
[2] *School of Mechanical and Electrical Engineering, Huainan Normal University, Huainan 232001, China*
[3] *School of Electrical and Communications Engineering, West Anhui University, Lu'an 237012, China*
[4] *School Electrical and Information Engineering, Hefei Normal University, Hefei 230061, China*

ABSTRACT: This paper presents a novel and compact single-layer patch filtering antenna with excellent out-of-band rejection performance. The antenna adopts a simple structure consisting of a single-layer substrate, a slot-loaded radiating patch, and a ground plane, and is fed by a coaxial probe. The rectangular radiating patch and ground plane are loaded with Γ-, anti-Γ-, and U-shaped slots to form the final design. The introduction of these slots successfully generates two resonance points, which extend the operating bandwidth. It also produces two out-of-band radiation nulls that enhance the out-of-band rejection performance. To validate the proposed design, antenna prototypes were fabricated and measured. The simulation and measurement results are consistent. The antenna exhibits stable realized gain and excellent bandpass response. It achieves a peak realized gain of 8.82 dBi, an impedance bandwidth of 12.8%, and out-of-band rejection greater than 21.26 dB. These characteristics make the proposed patch antenna highly suitable for various wireless communication applications.

1. INTRODUCTION

With the rapid development of wireless communication technology, the demand is increasing for miniaturized designs and improved interference immunity in radio frequency (RF) equipment. In a typical RF front-end, the antenna and the band-pass filter (BPF) are usually designed as two separate components, which are typically connected via a 50-ohm connector. The antenna serves to transmit and receive electromagnetic signals, while the BPF functions to transmit desired signals and suppress unwanted signals in other frequency bands. Traditionally, antennas are cascaded with additional filtering elements to achieve bandpass filtering. Traditionally, antennas are cascaded with additional filtering elements to achieve bandpass filtering. However, directly connecting these two components not only results in higher insertion loss but also adds to the device's size and complexity. This degrades performance and increases the overall system footprint. As discussed in [1–3], the conventional approach of stand-alone design leads to complex circuitry, significant signal distortion, and increased losses. For these reasons, filtering antennas, which combine the filtering function of a filter with the radiation characteristics of an antenna, have emerged as an effective solution. This approach reduces the size of the RF device and enables additional functionality integration without compromising antenna performance. Among various types of filtering antennas, microstrip patch filtering antennas have been widely studied and applied due to their low profile, cost-effectiveness, ease of fabrication, and ease of integration.

Currently, filtering antenna design methods are generally categorized into three primary techniques. The first technique involves cascading antennas and filters via transmission lines [4–7]. This design approach employs connectors or impedance matching networks to link individually designed filters and antennas, forming a complete filtering antenna. In [4], a novel design is introduced that utilizes a single cavity to integrate both the filter and antenna. This enables simultaneous filtering and radiation across three distinct frequency bands. However, the cascade design approach leads to a complex configuration and high fabrication costs. The second technique utilizes the final resonator of a multi-resonator coupled bandpass filter as the radiating element [8–10]. This approach overcomes many limitations of the cascade method. In [8], which avoids cascading, a corner-truncated patch is used as both the radiating element and the final resonator in the filtering network. This configuration introduces an additional radiation null and contributes to system miniaturization. However, its frequency selectivity remains limited. The third technique adopts a co-design approach to generate radiation nulls near the operating band. This is accomplished by introducing slots [11–14], adding parasitic patches [15–17], incorporating shorted vias [18–19], employing defected ground structures (DGS) [20–22], utilizing half-mode substrate-integrated waveguides (HMSIWs) [23–25], and stacking patches [26–29] to realize a desired filtering response. In most wideband filtering patch antenna designs, a combination of these techniques is commonly employed to attain both wide bandwidth and high out-of-band rejection.

In [13], a patch antenna with two pairs of rectangular slots is proposed to introduce two radiation nulls, which improves filtering performance but results in a relatively narrow impedance bandwidth. In [24], a low-profile filtering antenna with good sideband rejection is proposed. It incorporates five short-circuiting pins and a multifunctional single slot within a half-mode substrate-integrated waveguide (SIW), achieving a height

* Corresponding author: Hao Gui (2023200712@aust.edu.cn).

TABLE 1. Dimensions of filtering antenna: (mm).

Parameter	L	W	h	l_{feed}	l_1	l_2	l_3
Value	50	50	2.5	8.5	28.4	13.75	10.7
Parameter	l_4	l_5	l_s	w_1	w_2	w_3	w_4
Value	2	2.8	6.2	26.4	2.25	1.65	9
Parameter	w_5	w_s	g_1	g_2	g_3	g_4	g_s
Value	0.9	2.8	3.8	0.65	0.65	0.6	0.2

of only $0.0087\lambda_0$. Although it exhibits favorable filtering characteristics, the impedance bandwidth is limited to 2.5%, which limits its suitability for broadband applications. In [27], a stacked circularly polarized filtering patch antenna with controllable radiation nulls is presented. It achieves filtering by incorporating slots on both upper and lower patch surfaces. However, the stacked design results in increased profile and greater structural complexity. Therefore, achieving an optimal balance between radiation and filtering performance is a major challenge. This is especially true when aiming for a simple and compact configuration in the design of filtering antennas.

Compared with conventional design approaches, fusion design method eliminates the requirement for an independent filtering module. This approach significantly reduces insertion loss along the signal transmission path and minimizes the overall system size. At the same time, it maintains excellent filtering characteristics while preserving the antenna's radiation performance. In addition, wireless communication systems require higher spectral efficiency and enhanced interference suppression at higher frequency bands, particularly in the deployment of fifth-generation (5G) and next-generation sixth-generation (6G) networks. integration.

In this paper, a compact single-layer patch filtering antenna fed by a coaxial probe is presented. It features a novel and simple structure, small size, high gain, and excellent out-of-band rejection. By etching a pair of Γ-shaped slots and multiple U-shaped slots on the radiating patch and ground plane, the antenna generates two distinct resonance points within the passband. Additionally, it produces two radiation nulls on either side of the passband in the gain response. These features enhance the bandpass characteristics and improve out-of-band suppression. The U-shaped slot etched on the ground plane enhances the frequency selectivity of the low-frequency radiation nulls, thereby improving the overall antenna performance. A prototype antenna was fabricated and measured to validate the proposed antenna's radiation and filtering characteristics. The compact antenna measures 50 mm × 50 mm × 2.5 mm and exhibits smooth gain across a wide bandwidth of 7.15–8.13 GHz (12.8%). It achieves a peak realized gain of 8.82 dBi and an out-of-band rejection exceeding 21.26 dB. These characteristics demonstrate the antenna's superior radiation and filtering capabilities.

In complex wireless communication scenarios, the proposed antenna is well suited for the use in satellite systems, radar applications, and 5G millimeter-wave networks. In satellite communications, particularly within the Ku band, it supports high-capacity data transmission. In 5G millimeter-wave communications, it facilitates high-speed data delivery, enhancing network throughput and reducing latency. With its excellent filtering characteristics and high gain performance, the proposed antenna is suitable for applications that demand high integration and strong interference suppression. It holds great potential for next-generation RF front-end systems to support high-speed, high-capacity, and low-latency communication requirements.

2. FILTERING PATCH ANTENNA DESIGN

2.1. Antenna Configuration

Figure 1 illustrates the overall structure of the proposed filtering patch antenna, with key design dimensions indicated. The antenna is printed on a single dielectric substrate and includes a square patch loaded with slots, an SubMiniature version A (SMA) probe, and a ground plane etched with a U-shaped slot. The square patch at the center of the substrate serves as the sole radiating element, on which two pairs of identical slots and an inverted U-shaped slot are symmetrically arranged along the y-axis. In addition, the feed probe is positioned along the y-axis of symmetry and is slightly shifted along the positive y-direction. The dielectric substrate used in this design is FR-4, which has a relative permittivity (ε_r) of 4.4 and a loss tangent ($\tan\delta$) of 0.02. Table 1 lists the detailed geometric parameters of the optimized antenna.

2.2. Antenna Design Process

To clearly illustrate the design process and filtering mechanism of the proposed filtering antenna, three reference antennas are designed and labeled in Figure 2. They include a conventional square patch antenna (Ant. 1), a square patch antenna with a pair of straight slots (Ant. 2), and a square patch antenna with a U-shaped slot (Ant. 3). The initial structure, Ant. 1, features a simple square patch as its radiating element. However, this conventional design suffers from limited bandwidth and low out-of-band selectivity. To overcome these limitations and enhance both radiation and filtering capabilities, Ant. 2 is developed by etching a pair of straight slots along the y-axis into the patch of Ant. 1. Proper impedance matching is achieved by adjusting the feed position. Ant. 3 is derived from Ant. 2, in which the straight slots are replaced by Γ-shaped slots. Additionally, three U-shaped slots are introduced on the outer region of Γ-shaped slots, and their positions are optimized to improve performance. The final proposed filtering antenna (Ant. 4) is derived from Ant. 3. An additional U-shaped slot is etched into the ground plane to further enhance its filtering characteristics.

Figure 3 presents the simulated reflection coefficients (S-parameters) and the realized gain of the reference antennas as well as the proposed filtering antenna. As shown in Figure 3(a), Ant. 1 generates a single resonance at 7.4 GHz and exhibits acceptable radiation performance. However, as shown in Figure 3(b), Ant. 1 exhibits poor out-of-band rejection and lacks distinct filtering characteristics.

For Ant. 2, a distinct resonance point at 7.5 GHz is achieved by introducing a pair of straight slots into the radiating patch. This modification improves impedance matching and extends the operating bandwidth. Figure 3(b) shows that two radiation nulls appear on either side of the passband in the gain response

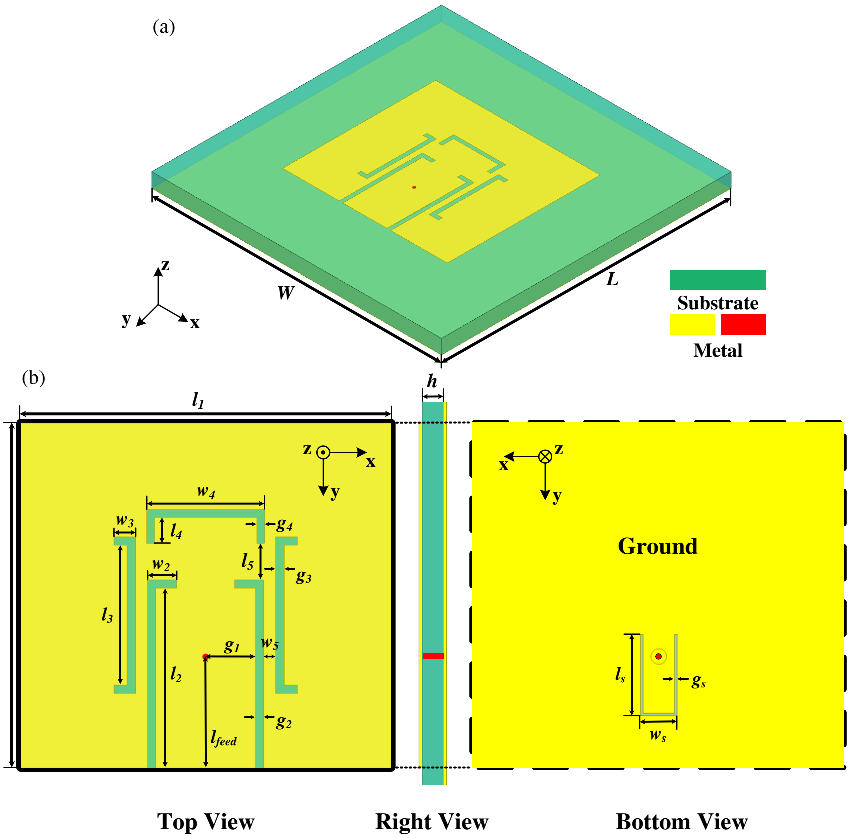

FIGURE 1. Geometry of the proposed filtering patch antenna. (a) Perspective view. (b) Top, right and bottom views.

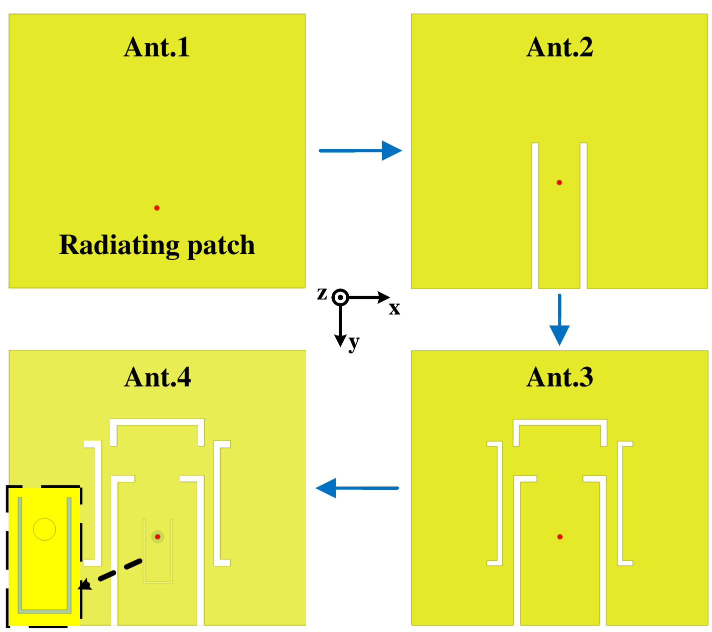

FIGURE 2. Evolution process of the proposed filtering antenna.

of Ant. 2. These nulls play a crucial role in enhancing the antenna's filtering performance. Compared with Ant. 1, Ant. 2 further extends the operating bandwidth (7.27–7.69 GHz) and demonstrates improved filtering performance. The gain outside the passband drops sharply from 8 dBi to below −5 dBi, indicating strong out-of-band suppression. However, the frequency selectivity at the band edges remains insufficient, and the gain response within the passband is uneven. Therefore, further enhancement of bandwidth and frequency selectivity is still necessary to improve overall antenna performance.

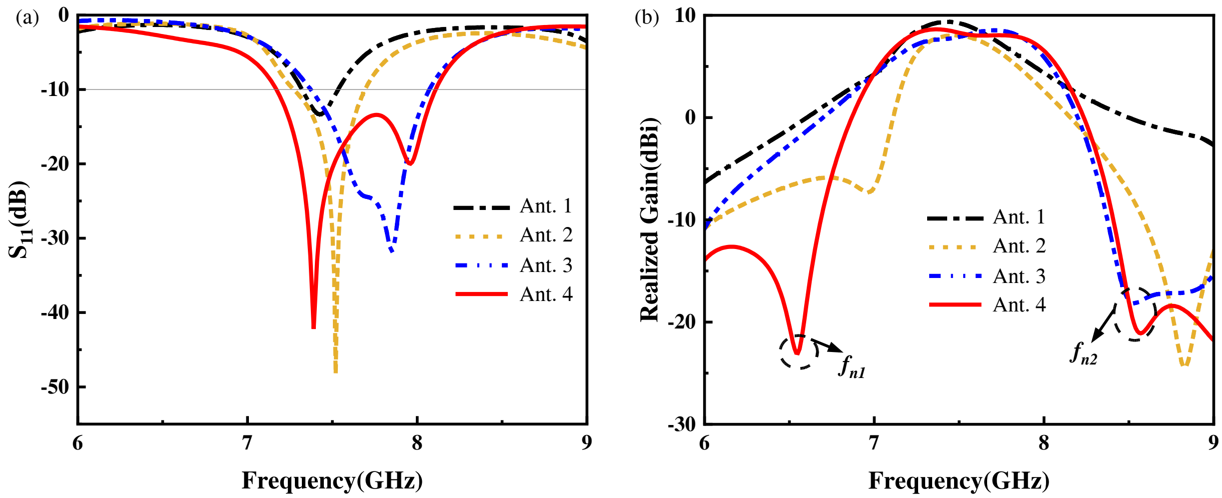

FIGURE 3. The S_{11} and realized gains of reference antennas and the proposed antenna (a) S_{11}. (b) Realized gains.

Ant. 3 is derived from Ant. 2 by replacing the straight slots with Γ-shaped slots. In addition, three U-shaped slots are strategically positioned around Γ-shaped slots to effectively enhance both radiation and filtering performance. Figure 3(a) shows that Ant. 3 generates an additional resonance at 7.85 GHz. It extends the antenna's operating bandwidth to approximately 5.6%, covering the range of 7.37–8.07 GHz. As shown in Figure 3(b), the frequency selectivity in the upper band is significantly improved, and the gain response within the passband becomes flatter. However, poor impedance matching at the lower-frequency resonance and the absence of radiation nulls in the lower stopband led to degraded frequency selectivity.

Finally, the proposed filtering antenna (Ant. 4) achieves two resonance points and two radiation nulls within the passband by etching a U-shaped slot in the ground plane of Ant. 3. According to the -10 dB return loss standard, Ant. 4 exhibits an impedance bandwidth of approximately 12.3% (7.17–8.11 GHz), as shown in Figure 3. It also achieves a peak realized gain around 8.65 dBi and maintains a stable gain response across the entire passband. As shown in Figure 3(a), the introduction of the U-shaped slot significantly improves impedance matching at the lower-frequency resonance. This modification enables the antenna to generate two distinct resonances at 7.39 GHz and 7.96 GHz, expanding the bandwidth to 7.17–8.11 GHz. As shown in Figure 3(b), a radiation null appears at 6.55 GHz in the lower stopband, resulting in an out-of-band rejection level exceeding 20 dB. This radiation null significantly enhances frequency selectivity in the lower stopband, demonstrating excellent filtering performance. Additionally, another radiation null appears at 8.57 GHz in the upper stopband, yielding an out-of-band rejection level exceeding 25 dB. Therefore, the proposed antenna provides a wide passband and strong out-of-band suppression characteristics.

2.3. Working Mechanism

To analyze the filtering performance of the proposed antenna, it is essential to clarify the mechanism responsible for generating radiation nulls. Figure 4 shows the surface current distribution of the proposed antenna at both the lower- and upper-frequency radiation nulls. The current distribution at the lower-frequency radiation null, f_{n1}, is shown in Figure 4(a). The currents are primarily concentrated in the inverted U-shaped slot of the radiating patch, two U-shaped slots, and U-shaped slot etched on the ground plane. These currents exhibit equal magnitudes but flow in opposite directions across the respective slots, forming a symmetrical distribution with respect to the y-axis. Similarly, the currents on either side of the U-shaped slot in the ground plane also flow in opposite directions with equal strength. As a result of the combined interaction between the radiating patch and ground plane, their opposing directions cause destructive interference, suppressing radiation. Consequently, a lower-frequency radiation null, f_{n1}, is formed at 6.55 GHz.

Figure 4(b) shows the surface current distribution at the high-frequency radiation null point, f_{n2}. The currents are primarily concentrated in the inverted U-shaped slot and the pair of Γ-shaped slots on the radiating patch. These currents exhibit equal amplitudes, flow in opposite directions, and are symmetrically distributed with respect to the y-axis on either side of the inverted U-shaped and Γ-shaped slots. As a result, the radiated fields cancel each other out, leading to the formation of the high-frequency radiation null, f_{n2}, at 8.57 GHz. Clearly, f_{n2} is generated through the combined effects of the inverted U-shaped and Γ-shaped slots.

Figures 4(c) and (d) illustrate the surface current distributions of the proposed antenna at the two resonant frequencies, $f_{z1} = 7.39$ GHz and $f_{z2} = 7.96$ GHz, respectively. At 7.39 GHz, the current is primarily concentrated on the radiating patch and around the Γ-shaped slots, indicating a perturbed fundamental mode. In contrast, at 7.96 GHz, strong current concentrations are observed around the inverted U-shaped slot and the Γ-shaped slots, forming additional current loops. These results confirm that the two resonant frequencies correspond to distinct radiating modes excited by the slot-loaded structure, which together broaden the impedance bandwidth and enhance the radiation performance.

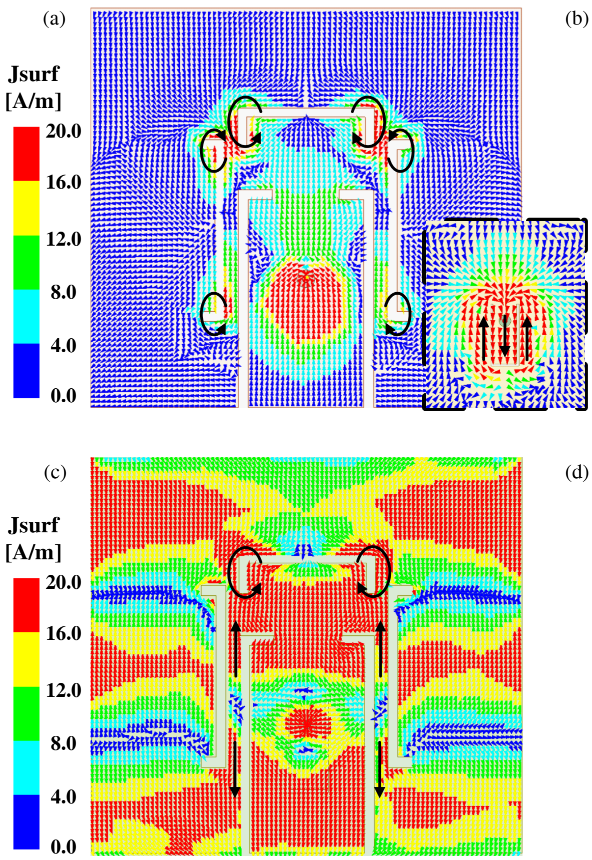

FIGURE 4. Surface current distributions of the proposed antenna at key frequencies: (a) $f_{n1} = 6.55$ GHz, (b) $f_{n2} = 8.57$ GHz, (c) $f_{z1} = 7.39$ GHz, and (d) $f_{z2} = 7.96$ GHz.

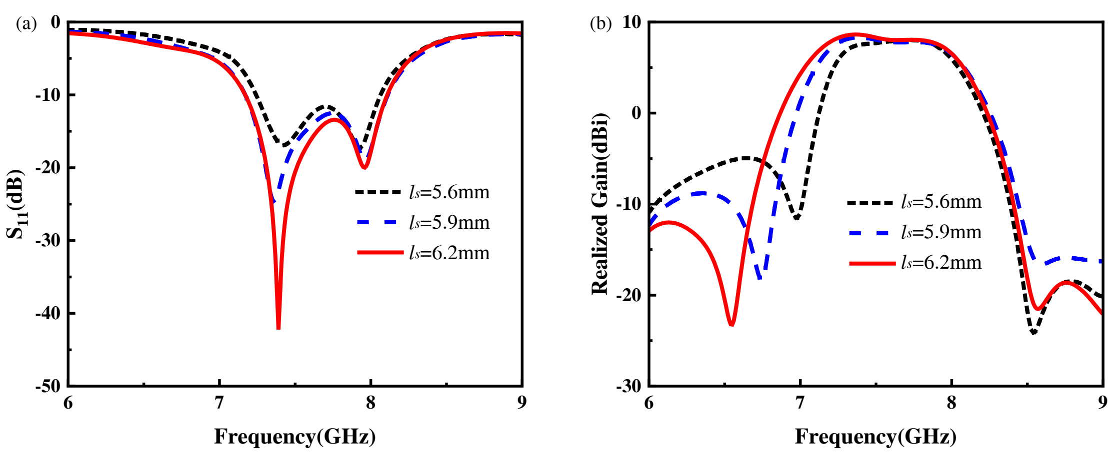

FIGURE 5. The S_{11} and realized gains at different lengths of l_s.

2.4. Controllability of Radiation Nulls

To further investigate the radiation null of the antenna, specific structural parameters are analyzed, as illustrated in Figures 5 and 6. The results indicate that the radiation null of the proposed filtering patch antenna can be effectively tuned by adjusting the key dimensions of the U-shaped slot. Figures 5 and 6 show the effects of varying these parameters on the reflection coefficient and realized gain, confirming that the position of the radiation null can be adjusted through structural optimization.

Figure 5 presents the simulated reflection coefficients and realized gains for different values of the U-shaped slot length (l_s) in the ground plane. As l_s increases from 5.6 mm to 6.2 mm, the lower-frequency radiation null (f_{n1}) shifts toward lower frequencies, resulting in enhanced out-of-band rejection performance. In contrast, the high-frequency radiation null f_{n2} remains largely unaffected. Moreover, Figure 5(a) indicates that variations in l_s have negligible effects on the resonance frequencies. Therefore, it can be concluded that the lower-frequency radiation null is primarily governed by the length of

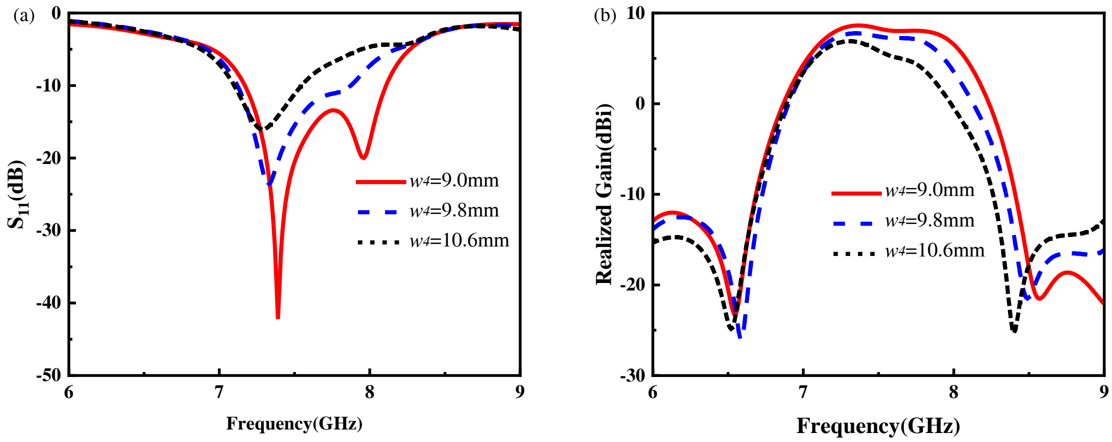

FIGURE 6. The S_{11} and realized gains at different lengths of w_4.

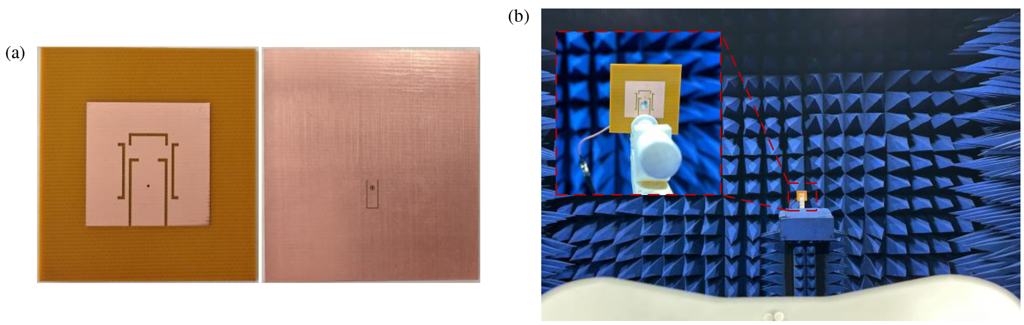

FIGURE 7. Photographs of (a) the fabricated proposed filtering patch antenna and (b) the measurement environment.

l_s, and its position can be effectively tuned by adjusting this parameter. A value of $l_s = 6.2$ mm is identified as the optimal design.

Similarly, Figure 6 illustrates the effects of varying the length (w_4) of the inverted U-shaped slot in the patch on the simulated reflection coefficients and realized gains. As shown in Figure 6(b), increasing w_4 from 9.0 mm to 10.6 mm causes the high-frequency radiation null (f_{n2}) to shift toward lower frequencies, while the lower-frequency radiation null (f_{n1}) remains nearly unchanged. Meanwhile, Figure 6(a) reveals that the high-frequency resonance point gradually shifts to lower frequencies as w_4 increases, whereas the lower-frequency resonance remains stable. The effect of the inverted U-shaped slot dimensions on the high-frequency resonance point can be calculated using the following equation:

$$f_{c2} = \frac{c}{2w_4 \times \sqrt{\varepsilon_r}} \tag{1}$$

where c denotes the velocity of the electromagnetic wave, and f_{c2} represents the resonant frequency of 7.96 GHz. Furthermore, as the slot length increases, the antenna's operational bandwidth narrows, and its impedance matching performance deteriorates. Therefore, it can be concluded that varying w_4 significantly influences the high-frequency radiation null and the impedance bandwidth of the antenna. A value of $w_4 = 9.0$ mm is identified as the optimal design.

3. MEASUREMENT AND COMPARISON

3.1. Antenna Model Measurement

The proposed patch filtering antenna was designed and simulated using High Frequency Structure Simulator (HFSS) electromagnetic simulation software. To further validate the design, a prototype of the proposed antenna was fabricated and experimentally tested. The fabricated antenna prototype is shown in Figure 7(a). Meanwhile, the S-parameters and radiation characteristics of the fabricated antenna were measured using a vector network analyzer and a microwave anechoic chamber, as illustrated in Figure 7(b).

Figure 8 presents both the simulated and measured S-parameters, realized gains, and radiation efficiency of the fabricated filtering antenna. As shown in Figure 8(a), the simulated and measured -10 dB impedance bandwidths are 12.3% (7.17–8.11 GHz) and 12.8% (7.15–8.13 GHz), respectively, with two distinct resonance points within the passband. The realized gain remains stable throughout the operating band. The simulated and measured peak realized gains are 8.65 dBi and 8.82 dBi, respectively. And the gain drops sharply below -20 dBi outside the passband, demonstrating the antenna's excellent filtering performance. Furthermore, two radiation nulls are observed at 6.55 GHz (6.53 GHz) and 8.57 GHz (8.52 GHz). The out-of-band rejection levels at the lower and upper frequencies are 20.65 dB (21.26 dB) and 27.27 dB (26.42 dB), respectively, further confirming superior

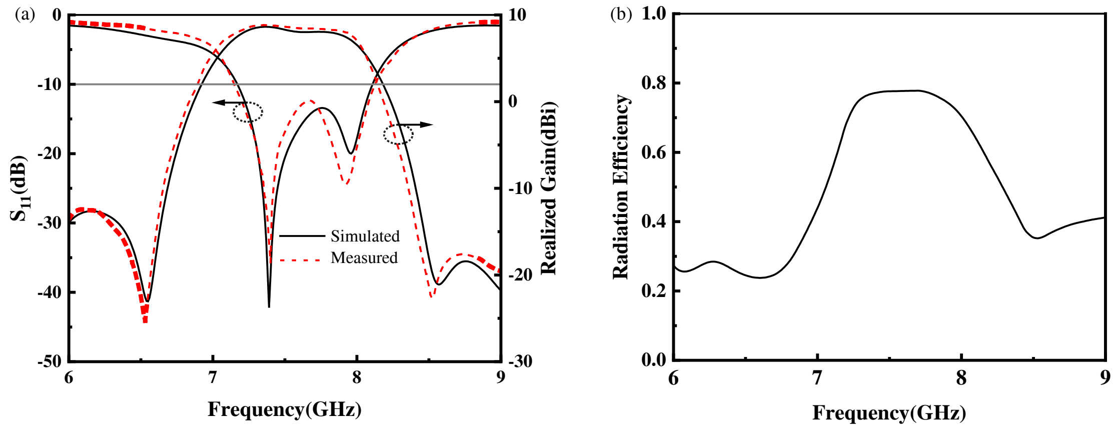

FIGURE 8. Simulated and measured reflection coefficients, realized gains, and radiation efficiency of the proposed filtering patch antenna. (a) Reflection coefficients and realized gains. (b) Simulated radiation efficiency.

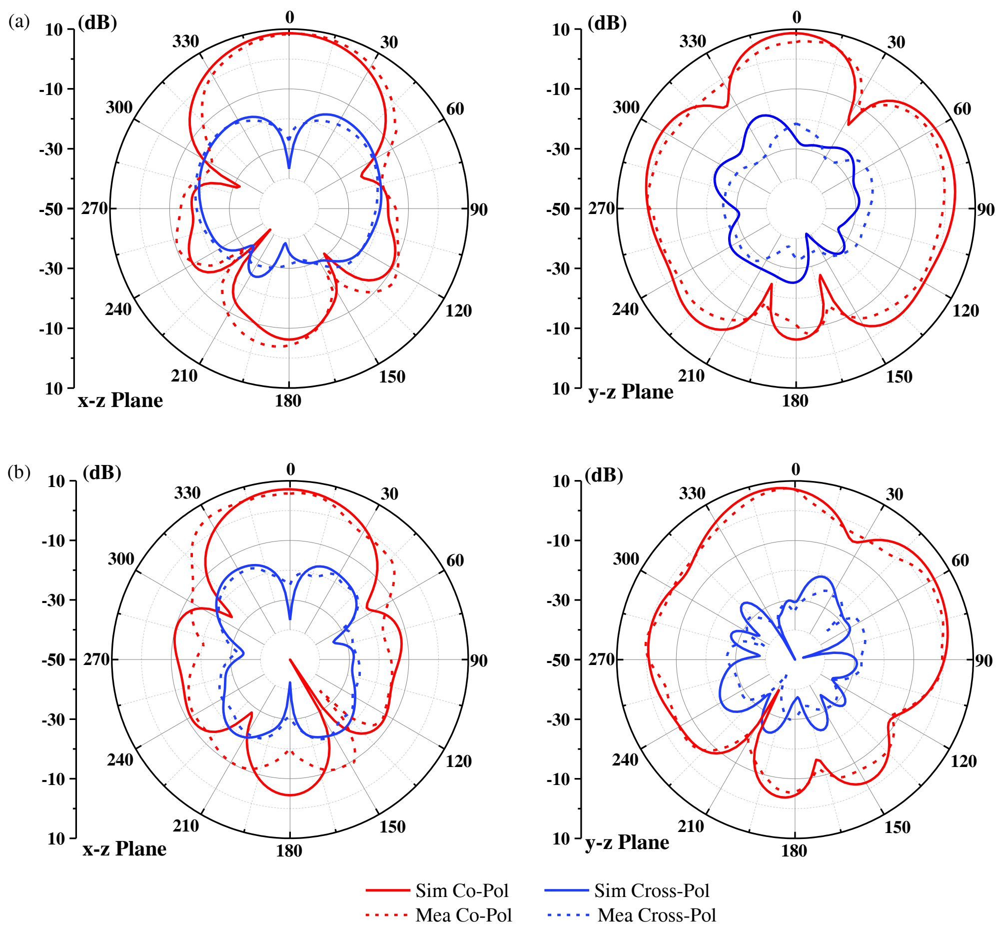

FIGURE 9. Simulated and measured radiation patterns of the filtering antenna at different frequencies. (a) 7.39 GHz, (b) 7.96 GHz.

filtering performance of the antenna. Moreover, the simulated radiation efficiency exceeds 70% across the entire operating band, whereas it remains relatively low outside the passband. Figure 9 shows the simulated and measured E-plane and H-plane radiation patterns at the two resonance frequencies of 7.39 GHz and 7.96 GHz. The antenna exhibits stable broadside radiation characteristics across the operating bandwidth. Moreover, good agreement is observed between the simulated and measured patterns, with consistently low cross-polarization levels. The co-polarization components dominate in the main radiation direction, while the cross-polarization suppression exceeds 20 dB, indicating good polarization purity. The measured front-to-back ratios are approximately 15.2 dB at 7.39 GHz and 17.1 dB at 7.96 GHz, confirming the antenna's radiation performance. Minor discrepancies between the simulated and measured results can be attributed primarily to

TABLE 2. Performance comparison of the filtering antennas.

Ref.	Extra element exclude slots	Size ($\lambda_0 \times \lambda_0$)	Bandwidth (%)	Gain (dBi)	Number of nulls	Suppression level (dB)	F_L/F_U
[8]	Yes	0.65×0.65	6.15	1.24	1	19.0	0.75/0.76
[12]	No	0.46×0.46	9.14	7.6	2	12.6	0.44/0.43
[17]	Yes	0.99×0.99	4.1	8.3	2	18.3	0.81/0.64
[21]	Yes	0.68×0.51	7.8	3.8	4	15.1	0.04/0.20
[24]	Yes	1.08×1.01	2.5	6.79	4	27.0	0.38/0.54
[29]	Yes	0.56×0.56	17.0	7.6	3	20.6	0.37/0.06
[26]	Yes	1.17×1.17	18.8	9.5	2	7.5	0.1/0.08
This letter	No	0.72×0.67	12.8	8.82	2	21.26	0.45/0.18

fabrication tolerances and slight variations in the measurement environment.

To further highlight the advantages of the proposed filtering patch antenna, Table 2 provides a performance comparison with other reported filtering antennas. In free space, λ denotes the wavelength corresponding to the center frequency f. The table also includes a comparison of frequency selectivity. The frequency selectivity at the lower and upper edges of the passband is calculated using the following equation.

$$F_L = \frac{f_{10L} - f_{15L}}{f_{10U} - f_{10L}}, \quad F_H = \frac{f_{15U} - f_{10U}}{f_{10U} - f_{10L}} \tag{2}$$

where f_{10L} and f_{10U} denote the lower and upper passband edge frequencies at which $S_{11} = -10$ dB, while f_{15L} and f_{15U} represent the lower and upper frequencies where the realized gain drops by 15 dB from that at the center frequency f. Smaller values of F_L or F_H indicate better frequency selectivity.

As shown in Table 2, the proposed filtering antenna exhibits significant advantages over previously reported designs in terms of structural simplicity, bandwidth, gain, and frequency selectivity. Compared with the antenna in [12], which solely employs slot structures, the proposed design achieves a wider bandwidth, higher gain, and enhanced out-of-band rejection. Although the antennas reported in [29] and [26] exhibit satisfactory radiation and filtering characteristics, they rely on multilayer architectures incorporating air layers and shorting vias, which increase fabrication complexity and production cost. In contrast, the proposed antenna is fabricated on a single-layer FR-4 substrate with printed metal patches. This design eliminates the need for additional components and meets the requirements for miniaturization and seamless integration into front-end systems. Compared with the filtering antennas in [8, 21, 24], the proposed design maintains a compact form factor while offering higher gain and broader bandwidth. Furthermore, it exhibits superior out-of-band rejection compared to the designs in [12, 21, 26], and better frequency selectivity than the antennas in [8, 17]. Although its bandwidth is not the most extensive among the designs listed, the overall performance remains comparable to or even superior to that of the existing counterparts. In summary, the proposed filtering antenna features wide bandwidth, high gain, strong out-of-band suppression, and excellent frequency selectivity. These features are achieved within a simple and compact structure, making the antenna suitable for front-end applications.

4. CONCLUSION

In this paper, a compact slot-loaded patch filtering antenna featuring high gain and excellent out-of-band rejection is proposed, fabricated, and experimentally validated. The antenna incorporates Γ-shaped, anti-Γ-shaped, and multiple U-shaped slots on the radiating patch and ground plane. They facilitate the generation of two resonance modes within the operating bandwidth. Simultaneously, two radiation nulls are introduced on either side of the passband, enhancing out-of-band suppression and frequency selectivity. The proposed design exhibits optimized in-band radiation characteristics along with superior out-of-band rejection performance. A prototype is fabricated and measured on a single-layer substrate without additional filtering structures, and demonstrates excellent performance. The proposed antenna achieves a peak gain of 8.82 dBi across a 12.8% bandwidth. The out-of-band rejection levels reach 21.26 dB and 26.42 dB in the lower and upper stopbands, respectively. These superior radiation and filtering characteristics make the proposed antenna a promising candidate for various applications, including wireless communication, satellite, and radar systems.

ACKNOWLEDGEMENT

This work was supported by the Fund of Anhui Mining Machinery and Electrical Equipment Coordination Innovation Center (Anhui University of Science and Technology) under grant No. KSJD202406.

REFERENCES

[1] Chen, X., M.-C. Tang, D. Li, and M. Li, "Flexible, bandwidth-enhanced, electrically small, electric near-field resonant parasitic antenna with filtering performance characteristics," *IEEE Transactions on Antennas and Propagation*, Vol. 70, No. 6, 4860–4865, Jun. 2022.

[2] Liu, S., Z. Wang, and Y. Dong, "A compact coupling-fed patch antenna with quasi-elliptic filtering response," *IEEE Antennas*

and Wireless Propagation Letters, Vol. 22, No. 12, 3137–3141, Dec. 2023.

[3] Choudhary, D. K., N. Mishra, P. K. Singh, and A. Sharma, "Miniaturized power divider with triple-band filtering response using coupled line," *IEEE Access*, Vol. 11, 27 602–27 608, 2023.

[4] Lin, J.-Y., S.-W. Wong, L. Zhu, Y. Yang, X. Zhu, Z.-M. Xie, and Y. He, "A dual-functional triple-mode cavity resonator with the integration of filters and antennas," *IEEE Transactions on Antennas and Propagation*, Vol. 66, No. 5, 2589–2593, May 2018.

[5] Deng, J., S. Hou, L. Zhao, and L. Guo, "Wideband-to-narrowband tunable monopole antenna with integrated bandpass filters for uwb/wlan applications," *IEEE Antennas and Wireless Propagation Letters*, Vol. 16, 2734–2737, 2017.

[6] Li, P., H. Chu, and R.-S. Chen, "Design of compact bandpass filters using quarter-mode and eighth-mode SIW cavities," *IEEE Transactions on Components, Packaging and Manufacturing Technology*, Vol. 7, No. 6, 956–963, Jun. 2017.

[7] Fakharian, M. M., P. Rezaei, A. A. Orouji, and M. Soltanpur, "A wideband and reconfigurable filtering slot antenna," *IEEE Antennas and Wireless Propagation Letters*, Vol. 15, 1610–1613, 2016.

[8] Wu, Z., A. Zhang, J. Chen, X. Lu, and J. Li, "Co-design of low profile single-fed circularly polarized filtering antenna with high out-of-band rejection," *AEU — International Journal of Electronics and Communications*, Vol. 102, 99–104, 2019.

[9] Choudhary, D. K. and R. K. Chaudhary, "Compact filtering antenna using asymmetric CPW-fed based CRLH structure," *AEU — International Journal of Electronics and Communications*, Vol. 126, 153462, Nov. 2020.

[10] Hong, W., Z.-J. Guo, and Z.-C. Hao, "Seamless integration technology for filtenna toward 5G/6G wireless communications," *IEEE Open Journal of Antennas and Propagation*, Vol. 5, No. 1, 18–36, Feb. 2024.

[11] Chen, X., L. Zhu, and M. Li, "Design of wideband, compact, filtering slot antennas enabled by mixed electric/magnetic couplings," *IEEE Transactions on Antennas and Propagation*, Vol. 72, No. 4, 3718–3723, Apr. 2024.

[12] Liu, Q. and L. Zhu, "A compact wideband filtering antenna on slots-loaded square patch radiator under triple resonant modes," *IEEE Transactions on Antennas and Propagation*, Vol. 70, No. 10, 9882–9887, Oct. 2022.

[13] Jin, J. Y., S. Liao, and Q. Xue, "Design of filtering-radiating patch antennas with tunable radiation nulls for high selectivity," *IEEE Transactions on Antennas and Propagation*, Vol. 66, No. 4, 2125–2130, Apr. 2018.

[14] Yang, W., Y. Zhang, W. Che, M. Xun, Q. Xue, G. Shen, and W. Feng, "A simple, compact filtering patch antenna based on mode analysis with wide out-of-band suppression," *IEEE Transactions on Antennas and Propagation*, Vol. 67, No. 10, 6244–6253, Oct. 2019.

[15] Li, L., H. D. Xiong, W. Y. Wu, A. B. Fu, and J. Y. Han, "A T-shaped strips loaded wideband filtering patch antenna with high selectivity," *IEEE Antennas and Wireless Propagation Letters*, Vol. 23, No. 1, 89–93, Jan. 2024.

[16] Hu, K.-Z., J. Yu, D. Li, Z. Chen, X. Chen, and D. Yan, "A single-layer low-profile frequency reconfigurable filtenna without extra filtering circuits," *IEEE Antennas and Wireless Propagation Letters*, Vol. 23, No. 12, 4583–4587, Dec. 2024.

[17] Yang, W.-J., Y.-M. Pan, and X.-Y. Zhang, "A single-layer low-profile circularly polarized filtering patch antenna," *IEEE Antennas and Wireless Propagation Letters*, Vol. 20, No. 4, 602–606, Apr. 2021.

[18] Zhang, X. Y., W. Duan, and Y.-M. Pan, "High-gain filtering patch antenna without extra circuit," *IEEE Transactions on Antennas and Propagation*, Vol. 63, No. 12, 5883–5888, Dec. 2015.

[19] Yang, W., M. Xun, W. Che, W. Feng, Y. Zhang, and Q. Xue, "Novel compact high-gain differential-fed dual-polarized filtering patch antenna," *IEEE Transactions on Antennas and Propagation*, Vol. 67, No. 12, 7261–7271, Dec. 2019.

[20] Cheng, G., J. Zhou, B. Huang, L. Yang, and Z. Huang, "Compact low-profile wideband filtering antenna without additional filtering structure," *IEEE Antennas and Wireless Propagation Letters*, Vol. 22, No. 10, 2477–2481, Oct. 2023.

[21] Chen, X., Q. Zhuge, G. Han, R. Ma, J. Su, and W. Zhang, "A wideband harmonic suppression filtering antenna with multiple radiation nulls," *Progress In Electromagnetics Research Letters*, Vol. 112, 17–25, 2023.

[22] Yang, W., S. Chen, Q. Xue, W. Che, G. Shen, and W. Feng, "Novel filtering method based on metasurface antenna and its application for wideband high-gain filtering antenna with low profile," *IEEE Transactions on Antennas and Propagation*, Vol. 67, No. 3, 1535–1544, Mar. 2019.

[23] Xie, H.-Y., B. Wu, Y.-L. Wang, C. Fan, J.-Z. Chen, and T. Su, "Wideband SIW filtering antenna with controllable radiation nulls using dual-mode cavities," *IEEE Antennas and Wireless Propagation Letters*, Vol. 20, No. 9, 1799–1803, Sep. 2021.

[24] Li, L., D. Pang, Y. Feng, Q. Wang, and Z. Lei, "A low-profile third-order half-mode SIW filtering antenna with low H-plane cross polarization and good sideband suppression," *IEEE Antennas and Wireless Propagation Letters*, Vol. 18, No. 12, 2503–2507, Dec. 2019.

[25] Wang, C., X. Wang, H. Liu, Z. Chen, and Z. Han, "Substrate integrated waveguide filtenna with two controllable radiation nulls," *IEEE Access*, Vol. 8, 120 019–120 024, 2020.

[26] Yuan, H., F.-C. Chen, and Q.-X. Chu, "A wideband and high gain dual-polarized filtering antenna based on multiple patches," *IEEE Transactions on Antennas and Propagation*, Vol. 70, No. 10, 9843–9848, Oct. 2022.

[27] Cheng, G., B. Huang, Z. Huang, and L. Yang, "A high-gain circularly polarized filtering stacked patch antenna," *IEEE Antennas and Wireless Propagation Letters*, Vol. 22, No. 5, 995–999, May 2023.

[28] Liang, G.-Z., F.-C. Chen, H. Yuan, K.-R. Xiang, and Q.-X. Chu, "A high selectivity and high efficiency filtering antenna with controllable radiation nulls based on stacked patches," *IEEE Transactions on Antennas and Propagation*, Vol. 70, No. 1, 708–713, Jan. 2022.

[29] Da Liu, Q., Q. Dong, J. X. Wen, L. H. Ye, D.-L. Wu, and X. Y. Zhang, "Compact wideband patch filtenna with enhanced out-of-band suppression," *IEEE Antennas and Wireless Propagation Letters*, Vol. 22, No. 9, 2310–2314, Sep. 2023.